Catalysis Today 171 (2011) 52–59

Contents lists available at ScienceDirect

Catalysis Today

journal homepage: www.elsevier.com/locate/cattod

C–H bond activation of methane on M- and MO-ZSM-5 (M = Ag, Au, Cu, Rh and Ru) clusters: A density functional theory study

Mehmet Ferdi Fellah [a], Isik Onal [b,*]

[a] Department of Chemical Engineering, Yuzuncu Yil University, Van 65080, Turkey
[b] Department of Chemical Engineering, Middle East Technical University, Ankara 06531, Turkey

ARTICLE INFO

Article history:
Received 28 August 2010
Received in revised form 3 April 2011
Accepted 4 April 2011
Available online 5 May 2011

Keywords:
DFT
Methane
C–H bond activation
Screening of catalytic activity
Metal
Metal–oxygen
ZSM-5
MFI

ABSTRACT

Density functional theory (DFT) calculations were carried out in a study of C–H bond activation of methane on [$(SiH_3)_4AlO_4$(M, MO)] (where M = Ag, Au, Cu, Rh and Ru) cluster models representing ZSM-5 surfaces. The following activity order of clusters with respect to their activation barriers could be qualitatively classified: Au ≫ Rh > Cu = Ru > Ag for metal-ZSM-5 clusters and Ag > Cu > Au ≫ Rh > Ru for MetalO-ZSM-5 clusters. Therefore, activation barriers based on transition state calculations showed that Ag–O–, Cu–O– and Au–O-ZSM-5 clusters (4, 5, and 9 kcal/mol, respectively) are more active than all the other clusters for C–H bond activation of methane.

1. Introduction

Methane, the most plentiful component of natural gas, is a useful raw material for the synthesis of more valuable products such as ethylene, methanol or formaldehyde. The C–H bond activation of methane that is considered to be the rate-limiting step in catalytic methane partial oxidation has received a great deal of attention both experimentally and theoretically [1–3]. Methane activation has been studied experimentally [4–8] as well as theoretically [9] on metal-exchanged ZSM-5 by several research groups. M'Ramadj et al. [4] investigated catalytic combustion of methane on high copper loading of ZSM-5 catalysts. They reported that Cu-ZSM-5 catalyst is an active catalyst for methane oxidation. They also reported that CuO is the active site for methane oxidation. Solmosi et al. [5] studied decomposition of methane and its reaction with CO_2 on Rh-ZSM-5 catalyst. They proposed the following reaction steps for methane activation:

$$CH_4 \leftrightarrow CH_{3(a)} + H_{(a)} \quad (1)$$

$$CH_4 + O_{(a)} \leftrightarrow CH_{3(a)} + OH_{(a)} \quad (2)$$

where "a" represents adsorbed species.

Ag-ZSM-5 catalyst has also been investigated for methane activation [8], and also in the presence of ethane [6,7] or benzene [6]. However, methane activation has not been experimentally investigated on Rh-ZSM-5 and Ag-ZSM-5 without an oxidant.

The only theoretical study of methane activation on mononuclear metal exchanged ZMS-5 is the work carried out by Ding et al. [9]. They used a [$(Si(OH)_3)_4AlO_4Ag$] model cluster for C–H bond activation of methane. They reported that the isolated Ag^+ cation has a role in the activation of methane on Ag-ZSM-5. Binuclear sites (metal–μO–metal) for several metals including Fe, Au, Ag and Cu in ZSM-5 have been used for methane activation in our recent theoretical study [10]. Many metal exchanged ZSM-5 catalysts, including Fe-ZSM-5 [11], Co-ZSM-5 [11], Cu-ZSM-5 [12–15], Rh-ZSM-5 [16,17] Ag-ZSM-5 [18,19], Au-ZSM-5 [19,20] and Ru-ZSM-5 [17] are presently being considered active catalysts for N_2O decomposition due to their high activity. N_2O decomposes to $N_{2(g)}$ and $O_{(a)}$ on the metal site of metal exchanged ZSM-5 catalyst. N_2O decomposition step can be shown as:

$$N_2O_{(g)} + O^* \rightarrow N_{2(g)} + O^* \quad (3)$$

where * represents metal site. Metal–oxygen site is formed as a result of this reaction.

A major challenge or debate on understanding the activity of metal-ZSM-5 catalysts is about the nature of active sites in ZSM-5 zeolite. The extra framework metal species in the zeolite

* Corresponding author. Tel.: +90 312 210 2639.
E-mail address: ional@metu.edu.tr (I. Onal).

0920-5861/$ – see front matter © 2011 Elsevier B.V. All rights reserved.
doi:10.1016/j.cattod.2011.04.001

micropores can be present as mononuclear, binuclear, oligonuclear cationic species. Solans-Monfort and co-workers have used a $[(SiH_3)_2AlO_2(OH)_2Cu]$ model cluster for N_2O decomposition [15], NO decomposition [21] and NOx decomposition [22] on Cu-ZSM-5 catalyst. They have reported that Cu and CuO sites are stable in Cu-ZSM-5 clusters. A $[(SiH_3)_4AlO_4Cu]$ ZSM-5 cluster model has been used for NO decomposition in theoretical [23,24] and experimental [25] studies by Bell and co-workers. They mentioned that both Cu and CuO sites are active sites for NO decomposition. These sites have been also used for interaction of NO_2, H_2O, SO_2 and NO molecules in other theoretical studies using a $[(SiH_3)_2AlO_2(OH)_2Cu]$ cluster model [26–28] and an $[Al(OH)_4Cu]$ cluster model [29,30]. Zhanpeisov et al. [18] researched interaction of N_2O with Ag^+ ion-exchanged ZSM-5 experimentally and theoretically. They used FT-IR spectroscopy and several cluster models such as $[Al(OH)_4Ag]$, $[(Si(OH)_3)_2AlO_2(OH)_2Ag]$ and $[(Si(OH)_2)_5O_4AlO_2(OH)_2Ag]$ for N_2O decomposition. The sites of Ag and Ag–O formed by N_2O decomposition have been investigated in a theoretical study [19] using a $[(SiH_3)_2AlO_2(OH)_2Ag]$ cluster model. Simakov et al. [31] experimentally investigated CO oxidation on Au-ZSM-5 catalyst. They reported that Au sites in the Au-ZSM-5 catalyst are responsible for the high activity in CO oxidation [32]. Au sites in the Au-ZSM-5 catalyst have been also reported by Gao et al. [33] in their experimental study of characterization of Au-ZSM-5. Au site of Au-ZSM-5 catalyst has been theoretically investigated by Sierraalta et al. [34]. Au and Au–O sites have been also reported in some theoretical studies which use a $[(SiH_3)_2AlO_2(OH)_2Au]$ cluster model [15] and a $(Si_6AlO_{23}H_{14}Au)$ cluster model [20] by Sierraalta et al. Rh-ZSM-5 catalyst has been investigated for N_2O decomposition [14,15]. Kondratenko and co-workers [16] reported in an experimental study that N_2O reversibly adsorbs over Rh-ZSM-5 with subsequent decomposition of adsorbed N_2O species to gas-phase N_2 and surface mono-atomic oxygen species.

The aim of this study is to investigate and compare C–H bond activation of methane on metal-exchanged ZSM-5 clusters by use of density functional theory (DFT) calculations. A metal-exchanged ZSM-5 zeolite is modeled as a $[(SiH_3)_4AlO_4(M \text{ or } MO)]$ (M = Ag, Au, Cu, Rh and Ru) cluster. DFT calculations with B3LYP formalism using 6-31G(d,p) basis set for Si, Al, O, C and H atoms and LANL2DZ basis set for metal atoms are utilized to obtain energy profiles, equilibrium geometries, and transition state geometries.

2. Surface models and calculation method

All calculations in this study are based on DFT [35] as implemented in Gaussian 03 suit of programs [36]. To take into account the exchange and correlation, Becke's [37,38] three-parameter hybrid method involving the Lee, Yang, and Parr correlation functional (B3LYP) formalism [39] was used in this study. It has already been demonstrated that hybrid B3LYP method is a high-quality density functional method certainly for organic chemistry [40]. 6-31G(d,p) basis set was utilized for Si, Al, O, C and H atoms and the Los Alamos LANL2DZ effective core pseudo-potentials (ECP) basis set was used for all metal atoms. Very large nuclei and electrons near the nuclei are treated in an approximate way in the LANL2DZ pseudo-potential basis set via effective core potentials including some relativistic effects as given in Ref. [41].

A cluster modeling approach was used to simulate a representative portion of ZSM-5 zeolite stabilizing the extra framework metal and metal–oxygen species in this study. Previous studies in metal-modified ZSM-5 and ferrierite zeolites by Kachurovskaya et al. [42,43] revealed only minor quantitative differences between the results obtained using cluster and periodic modeling approach. In addition, cluster modeling approach has been widely used to create a qualitative molecular-level picture of CO and NO adsorption on different iron sites of Fe-ZSM-5 [44] and on Pd–H-ZSM-5 [45]. Very similar structural and energetic properties of the adsorption complexes were obtained using small 5 T and large 83 T cluster models [44]. Furthermore, 7 T and 93 T cluster models were found as equally efficient in terms of the adsorption of CO and NO molecules on Pd–H-ZSM-5 [45]. A more important issue is that DFT calculations on cluster or periodic zeolite models generally predict very similar reactivity trends [44,46–48].

In this study, a 5T-ZSM-5 cluster from the wall (see Fig. 1b) of ZSM-5 zeolite was used. The starting geometry of the cluster model corresponded to the experimental XRD structure of ZSM-5 [49]. The initial cluster model contained 5 Si and 4 O atoms. An Al atom was placed in T12 site of the framework surrounded by O and Si atoms to generate distant framework anionic sites resulting in a $[(SiH_3)_4AlO_4]^{1-}$ cluster model. The negative charge of the cluster was compensated by the extra framework reactive sites such as $[M]^{1+}$ and $[MO]^{1+}$ where metal has a formal charge of 3+. The 5T-ZSM-5 clusters used in this study were modeled as $[(SiH_3)_4AlO_4(M \text{ or } MO)]$ (where M = Ag, Au, Cu, Rh and Ru) as shown in parts c and d of Fig. 1, respectively. The dangling bonds of the terminal silicon atoms are terminated with H atoms to obtain a neutral cluster. Total charge value for all complex systems such as M-ZSM-5 cluster-methane and MO-ZSM-5 cluster-methane systems was taken to be neutral. All of the atoms of a cluster except terminating H atoms, as well as reactant and product molecules were kept relaxed. Terminating H atoms were kept fixed to orient in the Si–O direction of the next Si site. Zeolite micropore feature was not considered in this study. The reactive sites studied in our work are relatively localized. Although dispersion may affect the energy of the adsorbed states in zeolite [50], it was also not taken into account in the present study since only a qualitative screening of activity for C–H bond activation of methane on metal exchanged ZSM-5 zeolites has been investigated. This effect would likely be similar for each of these cluster systems and thus would not influence conclusions based on the screening of the ZSM-5 clusters. Moreover, it has been reported that dispersion energy terms are comparable for different metal exchanged zeolite systems [51]. Energy profile and equilibrium geometry calculations were in general performed for determination of activation barriers and relative energies. Energy values in this study include zero-point energy (ZPE) corrections which are obtained using frequency calculations at a temperature of 298 K since there is no experimental thermochemistry data for C–H bond activation of methane. Computed $\langle S^2 \rangle$ values confirmed that the spin contamination was very small (within 0.5% after annihilation). Vibrational analysis was performed by means of single point frequency calculations for all transition states in order to confirm that they have only one imaginary mode of vibration. Natural bond orbital (NBO) [52] analysis has been used to obtain NPA charges and electronic configurations of metal atoms. Convergence criteria which are gradients of maximum force, root-mean-square (rms) force, maximum displacement, and rms displacement in Gaussian'03 software are 0.000450, 0.000300, 0.001800 and 0.001200, respectively.

The computational strategy employed in this study is as follows: initially, the correct spin multiplicity (SM) of the cluster and adsorbing molecule is determined by single point energy (SPE) calculations. SPE's are calculated with different SM numbers for each cluster system and the SM number which corresponds to the lowest SPE is accepted as the correct SM. The cluster and the adsorbing molecule, CH_4, are then fully optimized geometrically by means of equilibrium geometry calculations.

The adsorbing molecule is first located over the active site of the cluster at a selected distance and a coordinate driving calculation is performed by selecting a reaction coordinate in order to obtain the variation of the relative energy with a decreasing reac-

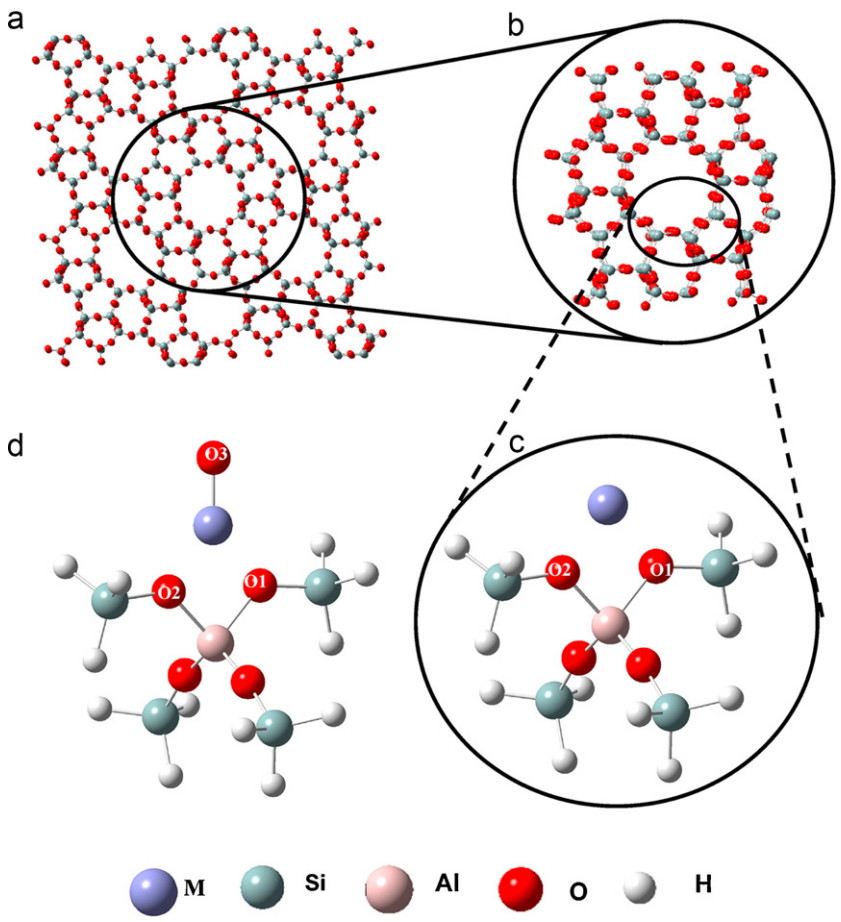

Fig. 1. (a) ZSM-5 zeolite, (b) ZSM-5 channel, (c) optimized geometries of M-ZSM-5 clusters, (d) optimized geometries of MO-ZSM-5 clusters (M = Ag, Au, Cu, Rh and Ru).

tion coordinate to get an energy profile as a function of the selected reaction coordinate distance. These energy profiles are also useful in finding transition state and equilibrium geometries. Single point energy calculations were also performed where necessary by locating the adsorbing molecule in the vicinity of the catalytic cluster. Coordinate driving calculations result in an energy profile. The resulting relative energies for the cluster and reactant molecule complex are plotted against the reaction coordinate. The relative energy is defined as the following formula:

$$\Delta E = E_{\text{System}} - (E_{\text{Cluster}} + E_{\text{Adsorbate}})$$

where E_{System} is the calculated energy of the optimized transition state or equilibrium structure, E_{Cluster} is the energy of the cluster, and $E_{\text{Adsorbate}}$ is that of the adsorbing molecule, CH_4 in this case. After obtaining the energy profile for the reaction step, the geometry with the minimum energy on the energy profile is fully re-optimized to obtain the equilibrium geometry for the particular reaction step. In this re-optimization calculation, the reaction coordinate is not fixed. Additionally, the geometry with the highest energy from the energy profile is taken as the input geometry for the transition state geometry calculations. Starting from these geometries, the transition state structures with only one negative eigenvalue in Hessian matrix are obtained. Transition states have been calculated using the synchronous quasi-Newtonian method of optimization, QST3 [53] in which reactant, product and a guess transition state structure are used. It has been reported that this method appears to be more reliable than conventional transition state optimization algorithms, and requires only energies and gradients, but not second derivative calculations [54]. Additionally, the computational cost of relaxing the path is less than or comparable to the cost of standard techniques for finding the transition state structures. It should be also noted that activation barrier values have been computed to be in well agreement with the experimental values using QST3 method in our theoretical studies [55,56] where benzene oxidation has been studied on Fe-ZSM-5 zeolite clusters.

3. Results

3.1. Optimization of clusters and reactant molecule

Equilibrium geometries for M- and MO-ZSM-5 clusters (M = Ag, Au, Cu, Rh and Ru) were obtained taking the total charge as neutral, and the calculated spin multiplicities corresponding to the lowest SPE's, respectively. Computed spin multiplicity (SM) numbers were shown in Table 1. The same spin multiplicity numbers for M- and MO-ZSM-5 clusters were also used for the cluster-methane molecule complex. The spin multiplicity numbers of 1 (singlet) and 3 (triplet) have been also reported for M- and MO-ZSM-5 clusters (where M = Ag and Au [19] and Cu [22]), respectively The parts c and d of Fig. 1 show geometries of a ZSM-5 cluster with a single M site and an MO site, respectively. Si–O distances for all clusters range from 1.63 Å to 1.68 Å. The corresponding distances reported in the experimental literature are between 1.55 Å and 1.65 Å [49]. Average Si–H distance was calculated as 1.485 Å for all clusters. NPA charges, the interaction energies of metal atoms with M-ZSM-5 cluster, distance values of M–O1, M–O2 and M–O3, and electronic configurations of metal atoms are reported in Table 1. Equilibrium geometry for CH_4 as a reactant molecule was obtained by taking the total charge to be neutral and with a singlet spin multiplicity. The calculated C–H bond distance value of 1.093 Å for methane

Table 1
NPA charges, interaction energies of metal atoms, selected distance values, and electron configurations of metal atoms of M- and MO-ZSM-5 clusters.

ZSM-5	Spin multiplicity	Distances (Å)			NPA charges				Interaction energy, kcal/mol	Electron configurations of metal atoms
		M–O1	M–O2	M–O3	Metal atom	Oxygen (O1) atom	Oxygen (O2) atom	Oxygen (O3) atom		
Ag	1	2.276	2.275	–	0.865	−1.316	−1.316	–	−78	$[core]5S^{0.13}4d^{9.97}5p^{0.01}6p^{0.02}$
Au	1	2.284	2.280	–	0.744	−1.279	−1.279	–	−71	$[core]6S^{0.30}5d^{9.92}6p^{0.02}7p^{0.02}$
Cu	1	2.006	2.003	–	0.864	−1.326	−1.326	–	−102	$[core]4S^{0.16}3d^{9.94}4p^{0.02}5p^{0.02}$
Rh	3	2.209	2.204	–	0.773	−1.284	−1.288	–	−89	$[core]5S^{0.09}4d^{8.11}5p^{0.02}$
Ru	4	2.212	2.120	–	0.787	−1.290	−1.292	–	−85	$[core]5S^{0.11}4d^{7.08}5p^{0.03}$
AgO	3	2.226	2.224	2.018	1.076	−1.304	−1.300	−0.279	–	$[core]5S^{0.22}4d^{9.67}5p^{0.04}$
AuO	3	2.237	2.230	1.885	0.995	−1.256	−1.256	−0.346	–	$[core]6S^{0.67}5d^{9.30}6p^{0.03}7p^{0.01}$
CuO	3	1.977	1.977	1.763	1.167	−1.300	−1.301	−0.415	–	$[core]4S^{0.35}3d^{9.44}4p^{0.03}$
RhO	3	2.128	2.105	1.723	1.029	−1.216	−1.262	−0.424	–	$[core]5S^{0.19}4d^{7.75}5p^{0.03}5d^{0.01}$
RuO	4	2.189	2.094	1.737	1.172	−1.213	−1.283	−0.543	–	$[core]5S^{0.22}4d^{6.57}5p^{0.04}5d^{0.01}$

molecule is very close to the reported experimental [57] value of 1.096 Å.

3.2. C–H bond activation of methane on M- and MO-ZSM-5 (M = Ag, Au, Cu, Rh and Ru) clusters

The proposed reactions [5] for the C–H bond activation of methane on a mononuclear site of M-ZSM-5 and MO-ZSM-5 clusters are:

$$\text{M-ZSM-5} + CH_{4(g)} \rightarrow CH_{3(M)} + H_{(Ob)} \quad (4)$$

$$\text{MO-ZSM-5} + CH_4(g) \rightarrow CH_{3(g)} + OH_{(M)} \quad (5)$$

where M represents the metal site and Ob is the bridge oxygen atom (O1) (see Fig. 1c).

3.2.1. C–H bond activation of methane on M-ZSM-5 (M = Ag, Au, Cu, Rh and Ru) clusters

For C–H bond activation of methane on M-ZSM-5 clusters, a reaction coordinate is the distance between the carbon atom (C) of the CH_4 molecule and the metal atom of the cluster. The relative energy profile for the activation on Ag-ZSM-5 cluster is shown in Fig. 2 to illustrate the methodology in obtaining the relative energy profiles. Tables 2 and 3 show NPA charge values and electronic configurations of metal atoms for equilibrium geometries and transition state geometries respectively for methane activation on M- and MO-ZSM-5 clusters. The transition states geometries and the equilibrium geometries for methane activation on M-ZSM-5 cluster are represented in parts a and b of Fig. 3, respectively.

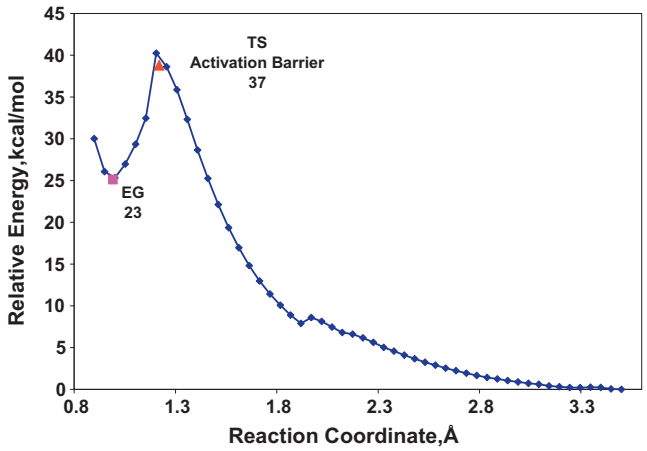

Fig. 2. Relative energy profile for C–H bond activation of methane on Ag-ZSM-5 cluster.

All geometries are similar for all metal exchanged ZSM-5 clusters. Table 4 shows geometric distance values for transition state and equilibrium geometry structures. Additionally, activation barriers, reaction energies and vibrational frequencies related with the transition mode for M-ZSM-5 clusters are tabulated in Table 6.

3.2.2. C–H bond activation of methane on MO-ZSM-5 (M = Ag, Au, Cu, Rh and Ru) clusters

A reaction coordinate is taken to be the distance between the hydrogen atom (H) of the CH_4 molecule and the adsorbed oxygen atom (O3 on metal atom) of the MO-ZSM-5 cluster for C–H bond activation reaction of methane which results in H adsorbed on O3 and CH_3 radical in the gas phase. Tables 2 and 3 show NPA charge values and electronic configurations of metal atoms for equilibrium geometries and transition state geometries respectively on M- and MO-ZSM-5 clusters. The transition state geometries and the equilibrium geometries for methane activation on MO-ZSM-5 cluster are represented in parts a and b of Fig. 4, respectively. All geometries are similar for all metal exchanged ZSM-5 clusters. Table 5 also shows geometric distances values for transition state and equilibrium geometry structures. Activation barriers, reaction energies and vibrational frequencies related with the transition mode for MO-ZSM-5 clusters are tabulated in Table 6.

4. Discussion

Since metal and MetalO sites have been determined in both experimental and theoretical studies in metal exchanged ZSM-5 [12–30], ZSM-5 clusters modeled as $[(SiH_3)_4AlO_4(M, MO)]$ (M = Ag, Au, Cu, Rh and Ru) are used for C–H bond activation of methane. Metal atoms interact chemically with ZSM-5 zeolite clusters by reason of their computed interaction energies shown in Table 1. The reason for this chemical interaction might be that the interaction between the negatively charged framework of a zeolite and the charge-compensating cations is primarily electrostatic and therefore quite strong and predominantly covalent [58]. NPA charge values and electronic configurations of metal atoms for equilibrium geometries and transition state geometries for methane activation on M- and MO-ZSM-5 clusters are shown in Tables 2 and 3, respectively. As seen from these tables, charge transfer occurs from the metal atoms and lattice oxygen atoms (O1 and O2) of zeolite to the adsorbing molecule for the reaction on M-ZSM-5 clusters whereas transfer takes place from the metal atoms and lattice oxygen atoms (O1 and O2) to the oxygen atoms (O3) on metals and adsorbing molecule during the reaction over MO-ZSM-5 clusters. The charges of metal atoms have decreased after breakage of C–H bond of methane on M- and MO-ZSM-5 clusters since ZSM-5 cluster has a Bronsted H site from methane. On the other hand, metal

Table 2
NPA charge values and electron configurations of metal atoms of transition state geometries for methane activation on M- and MO-ZSM-5 clusters.

ZSM-5 cluster	NPA charges				Electron configurations of metal atoms
	Metal	Oxygen (O1) atom	Oxygen (O2) atom	Oxygen (O3) atom	
Ag	0.755	−1.214	−1.316	–	$[core]5S^{0.29}4d^{9.94}6p^{0.02}$
Au	0.665	−1.244	−1.278	–	$[core]6S^{0.55}5d^{9.77}7p^{0.02}$
Cu	0.749	−1.219	−1.319	–	$[core]4S^{0.38}3d^{9.86}5p^{0.01}$
Rh	0.645	−1.227	−1.284	–	$[core]5S^{0.21}4d^{8.14}5p^{0.01}$
Ru	0.658	−1.220	−1.288	–	$[core]5S^{0.25}4d^{7.08}5p^{0.01}5d^{0.01}$
AgO	0.939	−1.284	−1.281	−0.502	$[core]5S^{0.33}4d^{9.70}5p^{0.03}$
AuO	0.942	−1.252	−1.256	−0.625	$[core]6S^{0.65}5d^{9.37}6p^{0.03}7p^{0.01}$
CuO	1.172	−1.302	−1.303	−0.700	$[core]4S^{0.35}3d^{9.44}4p^{0.03}$
RhO	0.930	−1.242	−1.187	−0.699	$[core]5S^{0.23}4d^{7.82}5p^{0.02}5d^{0.01}$
RuO	1.179	−1.283	−1.280	−0.832	$[core]5S^{0.29}4d^{6.50}5p^{0.03}5d^{0.01}$

Table 3
NPA charge values and electron configurations of metal atoms of equilibrium geometries for methane activation on M- and MO-ZSM-5 clusters.

ZSM-5 cluster	NPA charges				Electron configurations of metal atoms
	Metal	Oxygen (O1) atom	Oxygen (O2) atom	Oxygen (O3) atom	
Ag	0.397	−1.183	−1.302	–	$[core]5S^{0.77}4d^{9.82}6p^{0.01}$
Au	0.293	−1.144	−1.289	–	$[core]6S^{1.04}5d^{9.66}7p^{0.01}$
Cu	0.515	−1.140	−1.308	–	$[core]4S^{0.69}3d^{9.78}5p^{0.01}$
Rh	0.443	−1.163	−1.293	–	$[core]5S^{0.44}4d^{8.11}5p^{0.01}$
Ru	0.471	−1.164	−1.291	–	$[core]5S^{0.63}4d^{6.90}5p^{0.01}5d^{0.01}$
AgO	0.960	−1.271	−1.282	−0.710	$[core]5S^{0.32}4d^{9.68}5p^{0.03}6p^{0.01}$
AuO	0.949	−1.246	−1.252	−0.813	$[core]6S^{0.65}5d^{9.37}6p^{0.03}7p^{0.01}$
CuO	1.199	−1.300	−1.302	−0.937	$[core]4S^{0.34}3d^{9.42}4p^{0.04}5p^{0.01}$
RhO	0.924	−1.237	−1.187	−0.842	$[core]5S^{0.24}4d^{7.80}5p^{0.03}5d^{0.01}$
RuO	1.170	−1.290	−1.280	−0.938	$[core]5S^{0.30}4d^{6.49}5p^{0.03}5d^{0.01}6p^{0.01}$

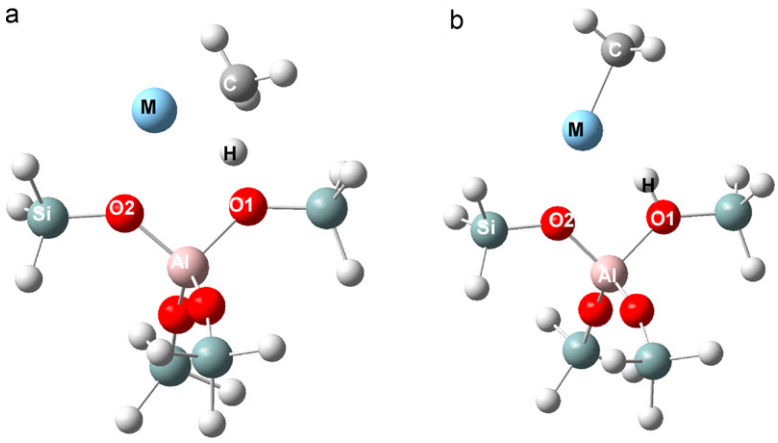

Fig. 3. (a) Transition state geometry and (b) equilibrium geometry for C–H bond activation of methane on M-ZSM-5 cluster (M = Ag, Au, Cu, Rh and Ru).

Table 4
Selected distance values of transition state geometries and equilibrium geometries for methane activation on M-ZSM-5 clusters (values are in units of Å).

M-ZSM-5 cluster	Transition state geometry			Equilibrium geometry		
	M–O2	O1–H	C–H	M–O2	M–C	O1–H
Ag	2.304	1.219	1.520	2.314	2.097	0.991
Au	2.203	1.489	1.477	2.301	2.034	1.001
Cu	1.950	1.222	1.559	2.002	1.913	1.001
Rh	2.215	1.299	1.501	2.317	2.075	1.026
Ru	2.237	1.258	1.540	2.340	2.080	1.025

Table 5
Selected distance values of transition state geometries and equilibrium geometries for methane activation on MO-ZSM-5 clusters (values are in units of Å).

MO-ZSM-5 cluster	Transition state geometry					Equilibrium geometry			
	M–O1	M–O2	M–O3	O3–H	C–H	M–O1	M–O2	M–O3	O3–H
Ag	2.237	2.253	2.049	1.223	1.299	2.250	2.228	2.058	0.977
Au	2.275	2.216	1.941	1.199	1.327	2.269	2.208	1.958	0.986
Cu	1.988	1.988	1.783	1.229	1.287	1.987	1.985	1.783	0.979
Rh	2.087	2.097	1.859	1.120	1.436	2.090	2.084	1.894	0.999
Ru	2.224	2.221	1.866	1.104	1.449	2.293	2.187	1.910	0.992

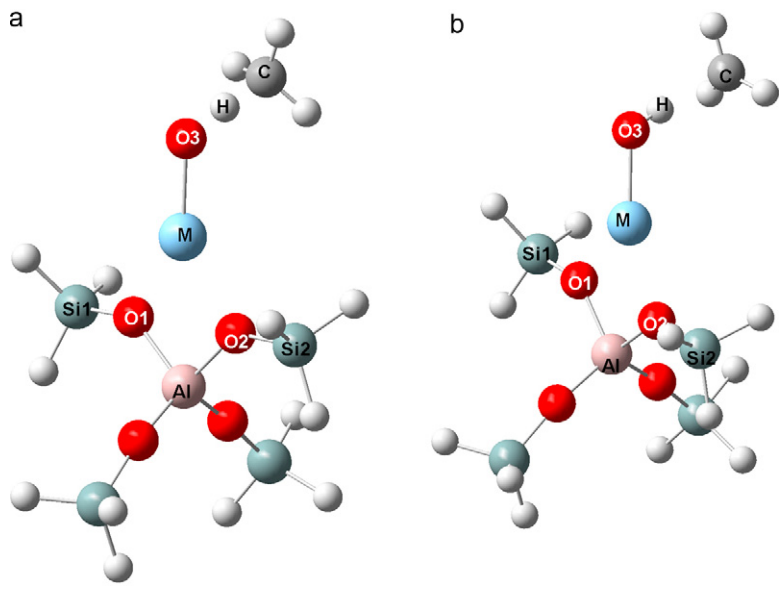

Fig. 4. (a) Transition state geometry and (b) equilibrium geometry for C–H bond activation of methane on M-ZSM-5 clusters (M = Ag, Au, Cu, Rh and Ru).

atoms in ZSM-5 clusters have already a positive charge at the end of C–H bond activation reaction. A comparison of the activation barriers and relative reaction energies for metal- and MetalO-ZSM-5 clusters is given in Table 6. Figs. 5 and 6 also summarize the energy diagrams of C–H bond activation of methane reaction on M- and MO-ZSM-5 clusters, respectively. As seen from Table 6 and Fig. 5, metal-ZSM-5 clusters except Au-ZSM-5 have similar heat effects on C–H bond activation of methane. Since NPA charge value of Au atom in the transition state geometry for Au-ZSM-5 cluster is lower than those of other metal-ZSM-5 clusters, Au-ZSM-5 cluster has a lower activation barrier value for C–H bond activation of methane than those of other ZSM-5 clusters. The reason for this difference between the activation barriers for Au-ZSM-5 cluster and other M-ZSM-5 clusters might be that in transition state mode of Au zeolite cluster the distance of H–O1 is much greater than those of other modes. Accordingly, a decrease in the number of electrons in the d orbital of the transition state mode for Au-ZSM-5 cluster is more than those of other M-ZSM-5 clusters. The methyl radical is strongly adsorbed on Au atom since Au atom has the lowest NPA charge after the C–H bond activation on Au-ZSM-5 cluster as compared to other metal-ZSM-5 clusters. Moreover, maximum charge decrease occurred on Au atom during the reaction. In order to see the reason for different heat effects on that reaction, desorption barriers of the methyl radical adsorbed on metal atom were calculated for Ru-ZSM-5 and Au-ZSM-5 clusters. Since Rh-, Ru-, Ag-, and Cu-ZSM-5 clusters have similar effects, Ru-ZSM-5 cluster was selected to compare with Au-ZSM-5 cluster. Desorption barrier values of the methyl radical from the surface for Ru-ZSM-5 and Au-ZSM-5 clusters were calculated to be 71 and 112 kcal/mol, respectively. Energy difference of these desorption barriers is calculated to be 41 kcal/mol. This is in reasonable agreement with the energy difference value of 45 kcal/mol calculated between reaction energy values for Ru- and Au-ZSM-5 clusters. Consequently, Au-ZSM-5 gives only exothermic heat effect for C–H bond activation.

Neither experimental nor theoretical literatures have activation barrier data for C–H bond activation of methane on M-ZSM-5 or MO-ZSM-5 catalysts except Ag-ZSM-5 which was used in a theoretical study [9]. Metal-ZSM-5 clusters have high activation barriers for C–H bond activation of methane. Conversely, activation barriers of metal-oxide ZSM-5 clusters except RhO- and RuO-ZSM-5 are significantly lower than those of metal-ZSM-5 clusters. The activation barrier of the reaction for Ag-ZSM-5 cluster was calculated to be 37 kcal/mol which is close to a theoretical value of 34 kcal/mol reported by Ding et al. [9]. However, there is a small difference which could be originated due to different basis sets utilized. AgO-ZSM-5 cluster has the lowest activation barrier (4 kcal/mol) for C–H bond activation of methane among all the metal oxides studied. Au-ZSM-5 is more active than Ag-ZSM-5 and other M-ZSM-5 clusters. Although the activation barrier for Au-ZSM-5 cluster was calculated to be 25 kcal/mol, it is much higher than that (9 kcal/mol) of AuO-ZSM-5 cluster. This is a similar trend to the experimentally reported information that AuO is responsible for the high activity in CO oxidation [32]. CuO-ZSM-5 cluster has an activation barrier value of 5 kcal/mol for methane activation whereas the barrier is 36 kcal/mol for Cu-ZSM-5 cluster. Here, CuO is the active site as also reported in the experimental study of M'Ramadj et al. [4]. Activation barriers for Rh- and RhO-ZSM-5 clusters were found as 34 and 28 kcal/mol, respectively. This, of course, indicates lower

Table 6
A comparison of the reaction energies and activation barriers of the C–H bond activation of methane on metal- and MetalO-ZSM-5 clusters.

Metal	Metal-ZSM-5 cluster			MetalO-ZSM-5 cluster		
	Activation barrier, kcal/mol	TS frequency, cm^{-1}	Reaction energy, kcal/mol	Activation barrier, kcal/mol	TS frequency, cm^{-1}	Reaction energy, kcal/mol
Ag	37, 34[a]	1236i	23	4	1340i	−1
Au	25	1381i	−18	9	1485i	3
Cu	36	1175i	27	5	1404i	−3
Rh	34	1260i	24	28	1421i	24
Ru	36	1255i	27	33	1226i	31

[a] A theoretical value reported by Ding et al. [9].

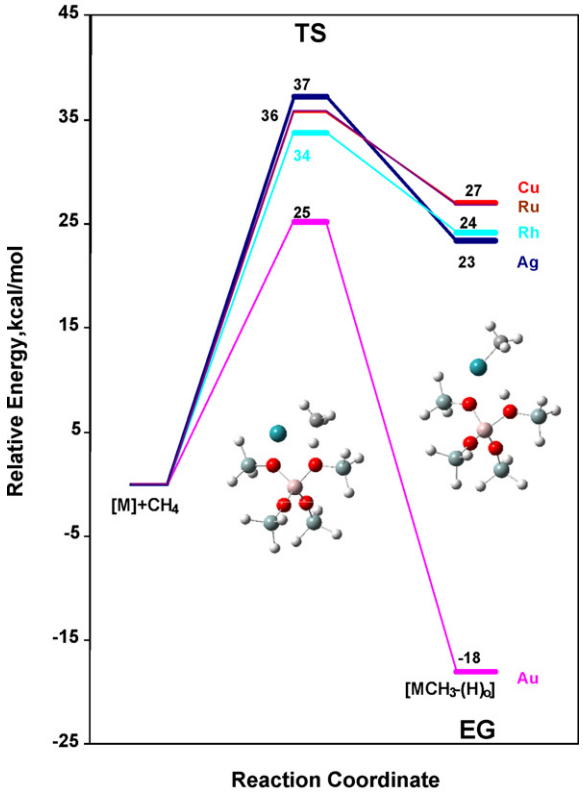

Fig. 5. A summary energy diagrams showing a comparison for C–H bond activation or methane on M-ZSM-5 clusters (M = Ag, Au, Cu, Rh and Ru).

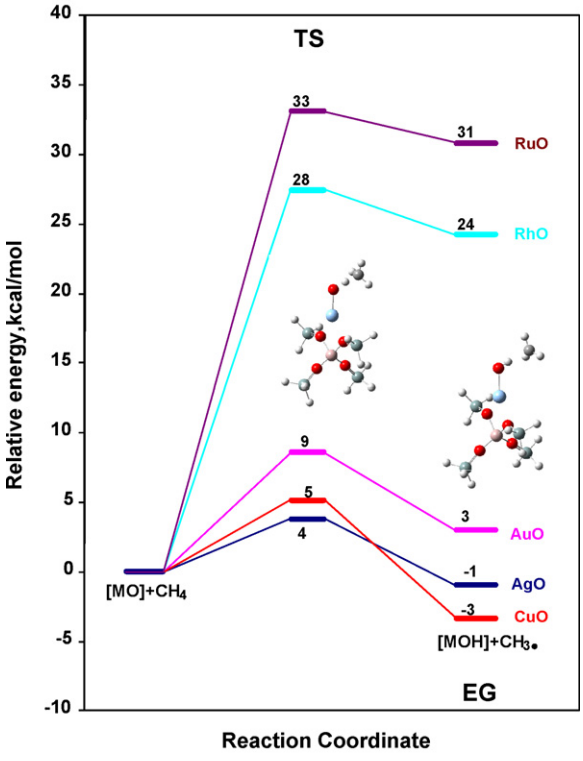

Fig. 6. A summary energy diagrams showing a comparison for C–H bond activation or methane on MO-ZSM-5 clusters (M = Ag, Au, Cu, Rh and Ru).

activity for Rh metal as compared to other metals located in a ZSM-5 cluster. These values are in agreement with the data given in an experimental study [5] which reports only 11.5% conversion of methane on Rh-ZSM-5 catalyst used for decomposition of methane and its reaction with CO_2. Clusters that exhibit the highest activation barriers for C–H bond activation of methane are Ru-ZSM-5 and RuO-ZSM-5 clusters. Activation barriers for these clusters were computed as 36 and 33 kcal/mol, respectively. Similar to the case of the M-ZSM-5 cluster discussed above, the explanation for the lower activation barriers of AgO-, AuO- and Cu-ZSM-5 clusters might be that in transition state modes of these clusters the H–O3 distance is greater than those of other modes.

As a result, the following activity order of clusters with respect to their activation barriers could be qualitatively classified: Au ≫ Rh > Cu = Ru > Ag for metal-ZSM-5 clusters and Ag > Cu > Au ≫ Rh > Ru for MetalO-ZSM-5 clusters. In view of these results, other possible reactions such as formation of methanol and/or formaldehyde can also be studied on AgO-, CuO- and AuO-ZSM-5 clusters.

5. Conclusions

The elementary reaction of C–H bond activation of methane on metal- and MetalO-ZSM-5 clusters modeled as $[(SiH_3)_4AlO_4(M, MO)]$ (M = Ag, Au, Cu, Rh and Ru) has been studied using DFT. The following activity order of clusters with respect to their activation barriers could be qualitatively classified: Au ≫ Rh > Cu = Ru > Ag for metal-ZSM-5 clusters and Ag > Cu > Au ≫ Rh > Ru for MetalO-ZSM-5 clusters. Activation barriers based on transition state calculations showed that AgO-, CuO- and AuO-ZSM-5 clusters are more active for C–H bond activation of methane as compared to other clusters.

Acknowledgments

This research was supported in part by TÜBİTAK (Scientific and Technical Research Council of Turkey) through TR-Grid e-Infrastructure Project. TR-Grid systems are hosted by TÜBİTAK ULAKBİM and Middle East Technical University (METU). Visit http://www.grid.org.tr for more information. This study was also partially supported by CENG HPC System of METU.

References

[1] M.F. Fellah, I. Onal, Turk. J. Chem. 31 (2007) 415–426.
[2] M.F. Fellah, I. Onal, J. Phys. Chem. C 114 (2010) 3042–3051.
[3] I. Onal, S. Senkan, Ind. Eng. Chem. Res. 36 (1997) 4028–4032.
[4] O. M'Ramadj, B. Zhang, D. Li, X. Wang, G. Lu, J. Nat. Gas Chem. 16 (2007) 258–265.
[5] F. Solmosi, A. Szöke, L. Egri, Top. Catal. 8 (1999) 249–257.
[6] T. Baba, K. Inazu, Chem. Lett. 35 (2006) 142–147.
[7] T. Baba, Catal. Surv. Asia 9 (2005) 147–154.
[8] Y. Kuroda, T. Mori, H. Sugiyama, Y. Uozumi, K. Ikeda, A. Itadana, M. Nagao, J. Colloid Interface Sci. 333 (2009) 294–299.
[9] B. Ding, S. Huang, W. Wang, Appl. Surf. Sci. 254 (2008) 4944–4948.
[10] E. Kurnaz, M.F. Fellah, I. Onal, Microporous Mesoporous Mater. 138 (2011) 68–74.
[11] M.F. Fellah, I. Onal, Catal. Today 137 (2007) 410–417.
[12] T. Goto, A. Niimi, K. Hirano, N. Takahata, S. Fujita, M. Shimokawabe, N. Takezawa, React. Kinet. Catal. Lett. 69 (2000) 375–378.
[13] V. Rakic, V. Rac, V. Dondur, A. Auroux, Catal. Today 110 (2005) 272–280.
[14] L. Chen, Y. Chen, J. Lin, K.L. Tan, Surf. Interface Anal. 28 (1999) 115–118.
[15] X.S. Monfort, M. Sodupe, V. Branchadell, Chem. Phys. Lett. 368 (2003) 242–246.
[16] E.V. Kondratenko, V.A. Kondratenko, M. Santiago, J.P. Ramirez, J. Catal. 256 (2008) 248–258.
[17] Y. Li, J.N. Armor, Appl. Catal. B 1 (1992) L21–L29.
[18] N.U. Zhanpeisov, G. Martra, W.S. Ju, M. Matsuoka, S. Coluccia, M. Anpo, J. Mol. Catal. A 201 (2003) 237–246.
[19] A. Sierraalta, R. Hernandez, E. Ehrmann, J. Phys. Chem. B 110 (2006) 17912–17917.
[20] A. Sierraalta, P. Alejos, E. Ehrmann, Int. J. Quantum Chem. 108 (2008) 1696–1704.
[21] X.S. Monfort, V. Branchadell, M. Sodupe, J. Phys. Chem. B 106 (2002) 1372–1379.
[22] X.S. Monfort, V. Branchadell, M. Sodupe, J. Phys. Chem. A 104 (2000) 3225–3230.
[23] L.B. Trout, A.K. Chekraborty, A.T. Bell, J. Phys. Chem. 100 (1996) 17582–17592.

[24] L.B. Trout, A.K. Chekraborty, A.T. Bell, J. Phys. Chem. 100 (1996) 4173–4179.
[25] A.W. Aylor, S.C. Larsen, J.A. Reimer, A.T. Bell, J. Catal. 157 (1995) 592–602.
[26] A. Sierraalta, R. Anez, M.R. Brussin, J. Phys. Chem. 106 (2002) 6851–6856.
[27] A. Sierraalta, A. Bermudez, M.R. Brussin, J. Mol. Catal. A 228 (2005) 203–210.
[28] A. Sierraalta, R. Anez, M.R. Brussin, J. Catal. 205 (2002) 107–114.
[29] W.F. Schneider, K.C. Hass, R. Ramprasad, J.B. Adams, J. Phys. Chem. B 101 (1997) 4352–4357.
[30] W.F. Schneider, K.C. Hass, R. Ramprasad, J.B. Adams, J. Phys. Chem. B 102 (1998) 3692–3705.
[31] A. Simakov, I. Tuzovskaya, A. Pestraykov, N. Bogdanchikova, V. Gurin, M. Avalos, M.H. Faries, Appl. Catal. A 331 (2007) 121–128.
[32] N.A. Hodge, C.J. Kiely, R. Whyman, M.R.H. Siddiqui, G.J. Hutchings, Q.A. Pankhurtst, F.E. Wagner, R.R. Rajaram, S.E. Golunski, Catal. Today 72 (2002) 133–144.
[33] Z.X. Gao, Q. Sun, H.Y. Chen, X. Wang, W.M.H. Sachtler, Catal. Lett. 72 (2001) 1–5.
[34] A. Sierraalta, P. Alejos, E. Ehrmann, L.J. Rodiguez, Y. Ferrer, J. Mol. Catal. A 301 (2009) 61–66.
[35] W. Kohn, L.J. Sham, Phys. Rev. 140 (1965) A1133–A1138.
[36] M.J. Frisch, G.W. Trucks, H.B. Schlegel, G.E. Scuseria, M.A. Robb, J.R. Cheeseman, J.A. Montgomery Jr., T. Vreven, K.N. Kudin, J.C. Burant, J.M. Millam, S.S. Iyengar, J. Tomasi, V. Barone, B. Mennucci, M. Cossi, G. Scalmani, N. Rega, G.A. Petersson, H. Nakatsuji, M. Hada, M. Ehara, K. Toyota, R. Fukuda, J. Hasegawa, M. Ishida, T. Nakajima, Y. Honda, O. Kitao, H. Nakai, M. Klene, X. Li, J.E. Knox, H.P. Hratchian, J.B. Cross, V. Bakken, C. Adamo, J. Jaramillo, R. Gomperts, R.E. Stratmann, O. Yazyev, A.J. Austin, R. Cammi, C. Pomelli, J.W. Ochterski, P.Y. Ayala, K. Morokuma, G.A. Voth, P. Salvador, J.J. Dannenberg, V.G. Zakrzewski, S. Dapprich, A.D. Daniels, M.C. Strain, O. Farkas, D.K. Malick, A.D. Rabuck, K. Raghavachari, J.B. Foresman, J.V. Ortiz, Q. Cui, A.G. Baboul, S. Clifford, J. Cioslowski, B.B. Stefanov, G. Liu, A. Liashenko, P. Piskorz, I. Komaromi, R.L. Martin, D.J. Fox, T. Keith, M.A. Al-Laham, C.Y. Peng, A. Nanayakkara, M. Challacombe, P.M.W. Gill, B. Johnson, W. Chen, M.W. Wong, C. Gonzalez, J.A. Pople, Gaussian 03, Revision D.01, Gaussian, Inc., Wallingford, CT, 2004.
[37] A.D. Becke, Phys. Rev. A 38 (1988) 3098–3100.
[38] A.D. Becke, M.R. Roussel, Phys. Rev. A 39 (1989) 3761–3767.
[39] C. Lee, W. Yang, R.G. Parr, Phys. Rev. B 37 (1988) 785–789.
[40] J. Baker, M. Muir, J. Andzelm, A. Scheiner, ACS Symp. Ser. 629 (1996) 342–367.
[41] J.B. Foresman, A. Frisch, Exploring Chemistry with Electronic Structure Methods, 2nd edition, Gaussian Inc., Pittsburgh, PA, 1996.
[42] N.A. Kachurovskaya, G.M. Zhidomirov, E.J.M. Hensen, R.A. van Santen, Catal. Lett. 86 (2003) 25–31.
[43] N.A. Kachurovskaya, G.M. Zhidomirov, R.A. van Santen, J. Phys. Chem. B 108 (2004) 5944–5950.
[44] M.F. Fellah, J. Phys. Chem. C 115 (2011) 1940–1951.
[45] B. Kalita, R.C. Deka, Catal. Lett. 140 (2010) 205–211.
[46] X. Rozanska, X. Saintigny, R.A. van Santen, F. Hutschka, J. Catal. 202 (2001) 141–155.
[47] X. Rozanska, R.A. van Santen, F. Hutschka, J. Hafner, J. Am. Chem. Soc. 123 (2001) 7655–7667.
[48] A.M. Vos, X. Rozanska, R.A. Schoonheydt, R.A. van Santen, F. Hutschka, J. Hafner, J. Am. Chem. Soc. 123 (2001) 2799–2809.
[49] H. Lermer, M. Draeger, J. Steffen, K.K. Unger, Zeolites 5 (1985) 131–134.
[50] C. Tuma, J. Sauer, Phys. Chem. Chem. Phys. 8 (2006) 3955–3965.
[51] X. Solans-Monfort, M. Sodupe, J. Ecker, J. Phys. Chem. C 114 (2010) 13926–13934.
[52] E.D. Glendening, A.E. Reed, J.E. Carpenter, F. Weinhold, NBO Version 3.1.
[53] C. Peng, H.B. Schlegel, Israel J. Chem. 33 (1993) 449–454.
[54] P.Y. Ayala, H.B. Schlegel, J. Chem. Phys. 107 (1997) 375–383.
[55] M.F. Fellah, R.A. van Santen, I. Onal, J. Phys. Chem. C 113 (2009) 15307–15313.
[56] M.F. Fellah, I. Onal, R.A. van Santen, J. Phys. Chem. C 114 (2010) 12580–12589.
[57] J. Andzelm, E. Wimmer, J. Chem. Phys. 96 (1992) 1280–1303.
[58] R.A. van Santen, M. Neurock, Introduction in Molecular Heterogeneous Catalysis, Wiley, Germany, 2006.